ANAS Transactions Earth Sciences 2 / 2023

http://www.journalesgia.com

SEISMIC ANALYSIS OF THE SHAMKIR RESERVOIR AREA THROUGH INSIGHTS INTO THE DYNAMICS OF THE EARTHQUAKE CHARACTERISTICS

Babayev T.H., Aliyev Y.N., Muradi I.B., Aliyev M.M.

Ministry of Science and Education of the Republic of Azerbaijan,
Institute of Geology and Geophysics, Azerbaijan
119, H.Javid Ave., Baku, AZ1143

Keywords: *the Shamkir water reservoir, the Middle Kur depression, b-value, Gutenberg-Richter law, intensity, ground motion, seismotectonic model*

Summary. This paper is dedicated to analyze the Shamkir reservoir area applying different tools using earthquake catalogs as a source to build up a long-term seismicity rate. The study area surrounds the western part of the Middle Kur depression and the north-eastern part of the Lesser Caucasus. The area covering 4300 km^2, is squeezed under seismic impact of mountainous zones such as the Greater Caucasus slope from the north and the northeastern part of the Lesser Caucasus from the south. The analysis was done estimating b-value, describing the relative distribution size of earthquake. Two catalogs of earthquakes were used to proceed the research: until 2015 with historical period (№1) and instrumental period between 1966-2018 (№2). b-value was estimated for each catalog defining M_c – magnitude of completeness, M_{max} – maximum magnitude and bins – magnitude steps on the Gutenberg-Richter linear relationship. For the catalogs №1 and №2, b-value was found 0.64 and 0.52, respectively. Furthermore, this study investigates the intensity distribution on the characteristic of earthquake faults computed by means of empirical relationship between maximum magnitude the source (faults) can generate and the length of the source (faults). The intensity that could be used to describe earthquake shaking in the northern part of the site of interest was observed as VII (MSK-64) and in the southern part as VIII.

© 2023 Earth Science Division, Azerbaijan National Academy of Sciences. All rights reserved.

Introduction

The study area is the Shamkir water reservoir region (Fig. 1) situated between the southern slope of the Greater Caucasus and the northern part of the Lesser Caucasus within the Eurasian plate and focusing on the area with location from (45.83 E, 41.14 N) to (46.61 E, 40.85 N) as a northern boundary and from (45.53 E, 40.67 N) to (46.30 E, 40.38 N) as the southern boundary and with the area of 4298.8 km^2 ~ 4300 km^2 (Babayev, Babayev, 2023). The core part of the structure is directed to the east in the form of a linear anticline, separates the Agjakend and Kepaz synclines and is interrupted by a transverse fault slide in the Tartar River bed (Alizadeh et al., 2016; Fig. 2).

The boundaries and the area of study zone is defined using ArcGIS 10.7 (ESRI, 2018) software. The purpose in this paper is to conduct the research of the seismicity applying empirical tools from the values in the appropriate earthquake catalogues, compute and estimate intensity shaking based on the faulting characteristics. We analyzed the seismicity regarding the assessment of the b-value of Gutenberg-Richter law and distribution of intensity through the study area generated by empirical ways.

Tectonics of the area

In the tectonic aspect, the region is categorized in two parts: the northern part of the site is a plain region being a part of the Middle Kur depression with the Pleistocene and Holocene sediments; the southern semi-zone of the site is a mountainous region containing mostly Middle Jurassic sediments. The northern region is included to Jeyranchol zone within Middle Kur mega-zone. The Middle Kur separates the southern slope of the Greater Caucasus and the northern part of the Lesser Caucasus (Bochud, 2011). The southern region of the research area is in the Lok-Karabakh zone within the Lesser Caucasus mountain-fold zone which is relatively seismically active (Alizadeh et al., 2016). In terms of stress orientation, the area is characterized by a dominant NNE-SSW-oriented compressional stress field which controls the overall occurrence of earthquakes and that most seismic events are represented by reverse faulting or strike-slip faulting (Tibaldi et.al., 2020; Babayev et.al., 2020a).

The Jeyranchol zone is located in the west of the Middle Kur depression (Alizadeh et al., 2016). It is bordered by the Lesser Caucasus zone in the south

along the Kur uplift. Three anticlines occur in the structure of the zone, the arch parts of them are disturbed by fault-overlaps (Alizadeh et al., 2016). It is divided into three belts: the Mammadtepe-Koyrukkeylan northern belt, the Ortagash-Quyrugenchi central belt and the Kur southern belt (Alizadeh et al., 2016). The Mammadtepe-Koyrukkeylan belt consists of Oglutepe, Mammadtepe, Saloglu, Garatepe, Gurzundag, Koyrukkeylan, South and North Jeyranchol and Tersdeller anticlines (Alizadeh et al., 2016). The Ortagash-Quyrugenchi belt covers Buyukkesik, Gushguna, western, central and eastern Ortagash, Quyrugenchi, Bayramli and Yenikend anticlines. The Kur belt contains Garayazi, Soyugbulag, Poylu, Zayam and Khuluf anticlines (Alizadeh et al., 2016).

The southern area of the research including the Lok-Karabakh zone is called Shamkir semi-zone which is the oldest and most complex structural element of the Lok-Karabakh zone that has passed the long tectonic development stage (Alizadeh et al., 2016). It consists of the Shamkir and Goygol uplifts in the west and east respectively. The Shamkir uplift is a huge heterogeneous and folded-block structure and is bounded by the Tovuzchay and Ganjachay transversal faults from the west and east respectively (Alizadeh et al., 2016). In its internal structure, the Central Shamkir and Lazılar-Arigdam uplifted blocks, which are secondary structures of the subregion and pan-Caucasus direction, and the Badakand and Gadabey downlifts, which border them from the north and south, respectively, are distinguished. The Goygol uplift is a south-westerly displacement continuation of the Shamkir uplift along the Ganjachay fault-slip. The core part of the structure is directed to the east in the form of a linear anticline, separates the Agjakend and Kepaz synclines and is interrupted by a transverse fault slide in the Tartar River bed (Alizadeh et al., 2016; Fig. 2). The geology of the study area changes from Mesozoic to Cenozoic according to the geological basemap we used in this research (Fig. 1). The southern zone mainly consists of Middle part of the Middle Jurassic (J_2^2). We also observe few amounts of rocks of the Lower Jurassic (J_1), intrusive rocks of the Middle and Upper Jurassic and Lower Cretaceous, and the rocks of the Upper part of the Middle Jurassic (Callovian) and Upper Jurassic (J_2^3-J_3), The Upper part of the Lower Cretaceous – Lower Paleocene (K_1^2-P_1^1) and very little section of the Pleistocene (Q_1^2-Q3) rocks laying from older to younger (Babayev, Babayev, 2023). According to Alizade et.al. (2016), these Jurassic sediments mainly contain volcanic, slightly less volcanic-sedimentary and sedimentary rocks. Alizade et.al. (2016) also proposes that in some places of Jurassic granites, granodiorites, diorites intrusions are spread. The northern zone consists of Pleistocene (Q_1^2-Q^3) rocks being more contemporary. Little sections of the Upper part of the Middle Jurassic (Callovian) and Upper Jurassic (J_2^3-J_3), the Upper part of the Lower Cretaceous – Lower Paleocene (K_1^2-P_1^1), Paleocene and Lower Eocene (P_1^2-P_2^1), Oligocene and Lower Miocene (P_3-N_1^1) are also spread over in this zone (Fig.1). Shamkir water reservoir is laid on the Holocene (Q_4) deposits. In this part of the area sediments are the "Agcagil" (N_2^2a) and continental layers and "Agcagil" (N_2^2a) sediments lie transgressively and under an angular unconformity on older rocks (Гадиров, 2012). The bottom of these sediments is represented by basal conglomerates. They do not appear on the surface. They consist of clays interspersed with sand and sandstone beds.

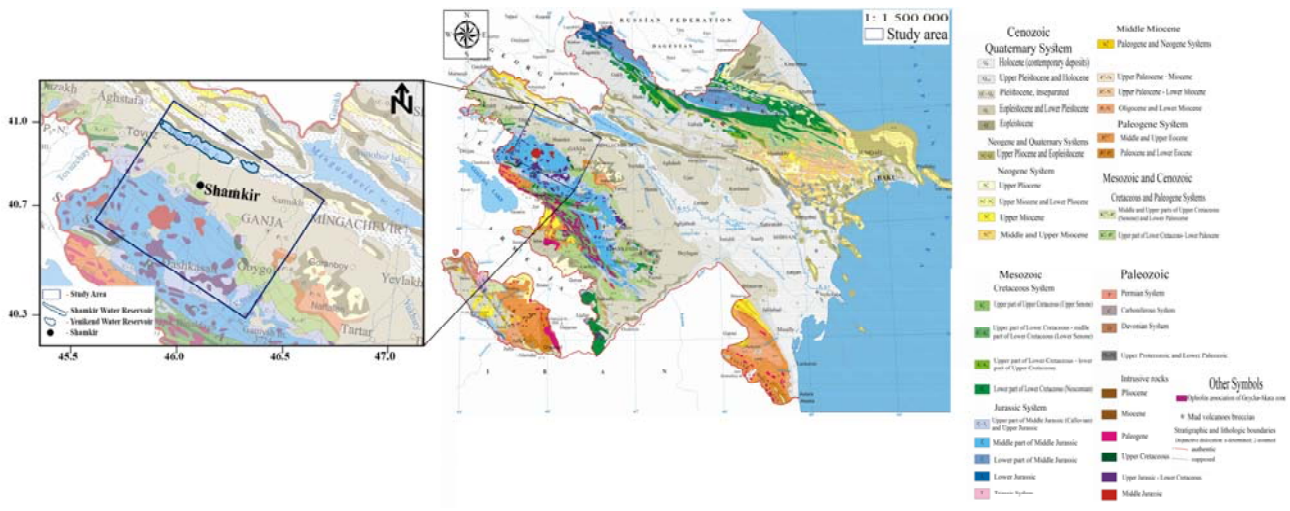


Fig. 1. The study area on geological map of Azerbaijan

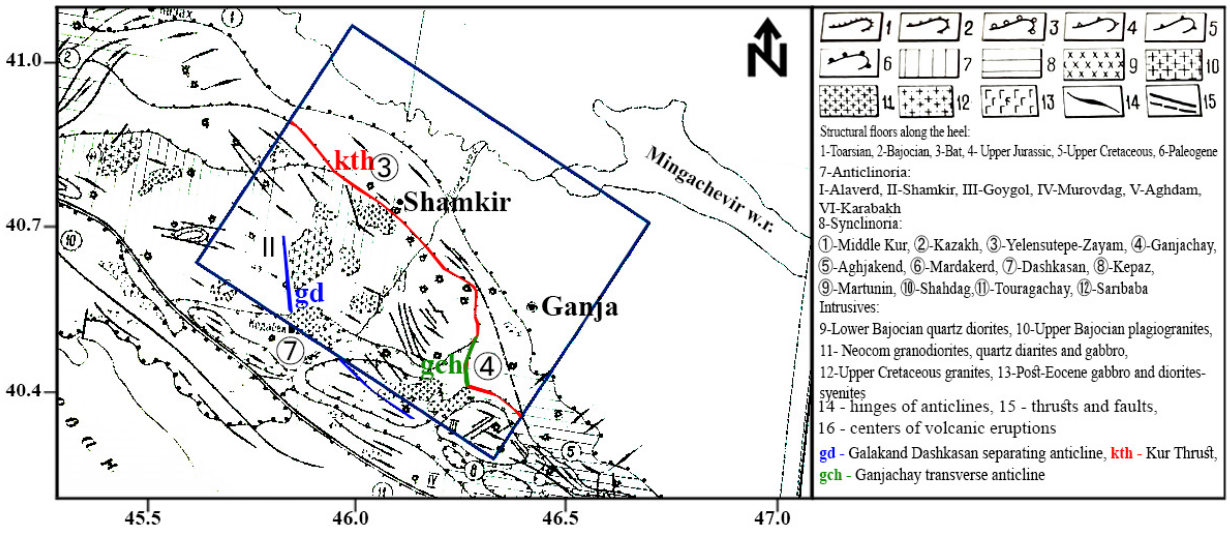


Fig. 2. Tectonics of the research area (Babayev, Babayev, 2023; Aliyev, 1961)

Methodology

Data selection criteria. To analyze the seismicity of the study area we have addressed two catalogs of seismicity (Table 1). The first is the earthquake catalog of Azerbaijan which involves the events registered between the years 427 and 2016. The next catalog is the earthquake catalog of Mingachevir region which is a region with high seismicity adjacent to the study area. It involves 1074 events registered between 1894 and 2018 years. We have filtered both catalogs with the criteria of compatibility to the study area. The procedure to filter the catalogs starts with use of ArcGIS 10.7 (ESRI, 2018) software. The events of the catalogs were illustrated on the map (Fig.7) according to their spatial distribution inside and outside the study area.

Thus, we worked with 1343 events in the first and 101 events in the second catalog. Tables 2 and 3 show selection from the catalogs.

As introduced in Table 1, we will name the catalog "EQ Catalogue_Azerbaijan 427-2016" as №1 and catalog "erqs Catalogue_Mingachevir 1894-2018" as №2.

Table 1

Used catalogs for the study area

Numeration of catalogs	Name of Catalogs	Number of events after filtration	Time range after filtration
№1	EQ Catalogue_Azerbaijan 427-2016	1343	427-2015
№2	erqs Catalogue_Mingachevir 1894-2018	101	1966-2018

Table 2

A fragment from "EQ Catalogue_Azerbaijan 427-2016"

Year	Day	Lat	Lon	H (km)	Mlh	K
427		40.5	46.5	12	6.7	15.7
1235		40.6	46.2	10	5.72	14.3
1826	25	40.7	46.2	15	4.3	11.7
1867	23	40.6	46.3	15	5.8	14.4
1900	18	40.6	46.4	12	4.4	11.9
1902	24	40.5	46.0	15	4.2	11.6
1903	18	40.7	46.4	12	4.6	12.1
1908	14	41.1	46.1	36	4.0	11.2
1910	18	40.7	46.3	18	4.5	12.1
1910	10	40.8	46.0	9	4.2	11.6
1929	11	40.4	46.2	15	3.9	11.0

Year	Day	Lat	Lon	H (km)	Mlh	K
1929	9	40.4	46.3	8	3.2	0
1931	8	40.7	46.3	20	4.3	11.7
1931	12	40.6	46.3	10	3.6	0
1939	4	40.8	46.7	22	3.6	0
1949	17	41.1	46.1	17	4.0	11.2
1962	12	41.0	45.9	5	4.2	11.6
1964	26	40.4	46.2	0	1.7	7.0
1964	1	40.6	45.9	0	2.2	8.0
1964	3	40.7	46.1	0	2.22	8.0
1964	8	40.9	46.0	0	2.5	8.5
1964	15	40.9	45.9	0	3.33	10.0
1964	27	40.8	46.1	0	2.78	9.0
1964	16	40.8	46.0	0	2.78	9.0

Mlh – magnitude of the earthquake; K – energy class of the earthquake

Table 3

A fragment from "erqs Catalogue_Mingachevir 1894-2018"

Year	mon	day	hours	second	Lat	Lon	H	Ml
1966	3	6	12	48	40.9	46.5	0	2.4
1976	8	10	10	21	40.8	46.6	0	2.4
1977	8	25	15	12	40.9	46.5	0	1.9
1978	7	16	21	48	40.9	46.6	0	1.9
1979	5	17	15	6	40.9	46.5	0	2.7
1980	11	21	15	31	40.9	46.4	0	1.3
1981	5	20	12	50	41.0	46.3	0	3.0
1981	10	6	14	58	40.9	46.5	0	2.4
1983	8	13	2	11	40.9	46.6	0	3.5
1985	5	24	6	8	40.8	46.6	10	2.0
1985	12	30	17	17	40.9	46.6	0	2.3
1986	2	6	0	20	40.87	46.4	0	1.9
1989	9	19	14	32	41.0	46.34	21	2.7
1990	4	13	3	57	40.91	46.55	32	2.7
1991	8	18	5	50	40.93	46.39	21	2.6
1992	6	2	18	54	41.0	46.25	0	2.5
1992	8	27	22	8	40.93	46.43	10	1.1
1994	9	20	6	34	40.9	46.5	0	2.5
2000	9	13	23	26	40.9	46.5	0	1.8
2001	2	28	23	3	40.9	46.35	0	2.6
2002	12	5	10	40	40.94	46.28	31	2.8
2003	2	5	1	0	40.85	46.51	14	2.3
2004	3	15	20	3	40.97	46.33	0	2.3
2005	1	29	11	40	40.98	46.39	23	2.2
2007	1	5	16	50	40.85	46.58	36	2.6

It is seen from the tables that depth for some events is set at 0. This case is mostly related to the low value of magnitude. It can be observed that for M=1.0 depth could be H=0.5-0.8 km, for M=3.0, H=1 km and for M=3.5, H=2 km (Цхакая, 1962; Varazanashvili, 1999). It concludes that those quakes occurred near- and sub-surface. Fig.3 illustrates the spatial distribution of magnitudes of earthquakes from the catalogs №1 (3a) and №2 (3b).

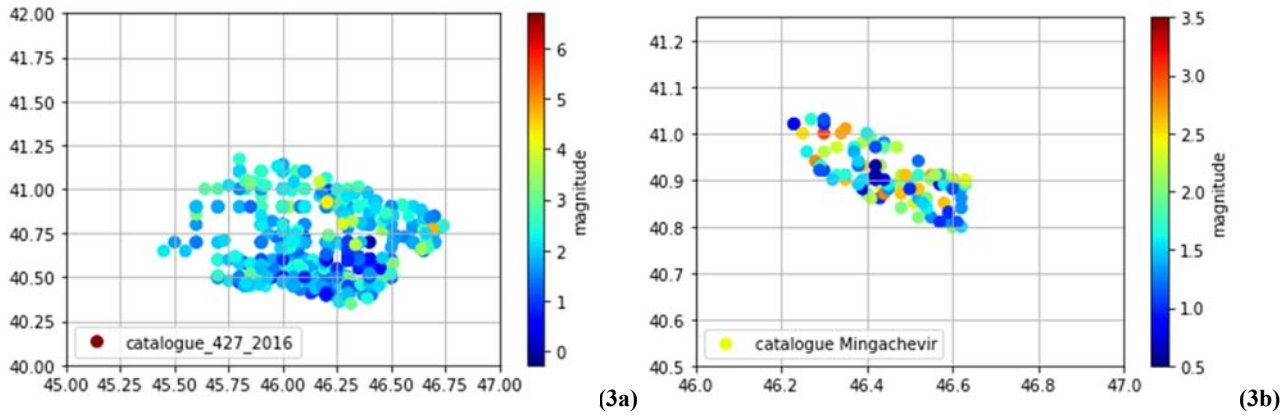


Fig. 3. Spatial distribution of magnitudes of earthquakes. (3a) catalog №1, (3b) catalog №2

Gutenberg-Richter Law. Richter (1935) proved that earthquakes are not uniformly distributed in time, space and magnitude. Earthquakes are distributed with respect to invariable scale of magnitudes being self-similar and obeying a power law or fractal scaling (Kulhanek, 2005). The distribution of earthquakes with respect to the magnitude is assessed by Gutenberg and Richter (1942) relation (GR law, briefly) – also known as Ishimoto and Iida (1939) – with the following empirical formula:

$$log\ N = a - bM \ \text{ or } \ N = \ 10^{a-bM}, \qquad (1)$$

where N is the number of earthquakes greater than and equal to M, the magnitude of the earthquakes, a and b are the real constants.

b-value estimation. "b" is the slope of the GR law equation. It is a parameter describing the relative size distribution of earthquakes. b-value is estimated by the following main techniques (El-Isa, Eaton, 2014):

- Linear least-square fit
- Maximum-likelihood estimation (Utsu, 1965):

$$b = log\ log\ \frac{e}{M_{av}-M_{min}} = \frac{0.43}{M_{av}-M_{min}}, \qquad (2)$$

where M_{av} is the mean of the observed magnitudes and M_{min} is the minimum magnitude – threshold magnitude in the events catalog. The relation above is defined for continuous distribution (Kulhanek, 2005).

In theory we expect similar results from these techniques, but empirically these methods do not necessarily yield the same b-values for the same seismicity data (El-Isa, Easton, 2014). For instance, El-Isa (2013) reports average differences in b-value about 0.1-0.2 between two methods based on analysis of global catalogs. Felzer (2007) points out: "In general, the least-square regression method may be disproportionately influenced by the largest earthquake magnitudes, whereas the maximum-likelihood method weights each earthquake equally". Some researchers such as Milojevic (2010), have mentioned that the least-square fitting to logarithmically binned data could be more preferable than the maximum likelihood method due to its instructivity (El-Isa, Eaton, 2014). In this research we decided to apply linear least-square fitting during estimation of b-value. The very first step in applying Gutenberg-Richter law (Gutenberg and Richter, 1942) for a catalog is to plot cumulative number of earthquakes in logarithmic scale respect to the magnitudes with N ≥ M where N – cumulative number of earthquakes and M – magnitudes (Fig. 4) to illustrate relation between the frequency of earthquakes and their magnitude. In the plot we apply linear regression method in order to find the slope of linearity and the intersection with the y-axis which are b- and a-values respectively due to the formula (1).

To apply the linear regression method, we have to correctly define M_c – magnitude of completeness, M_{max} – maximum magnitude till which the linear fit goes on (Godano et al., 2014; Godano et al., 2021), magnitude bin – simply the step for the magnitudes. For the catalog №1, M_c=3, M_{max}=4.8, bins=0.1 M_c, M_{max}, bins were defined as 3.0, 4.8, 0.1 respectively and for №2 as 1.0, 2.6, 0.1 respectively.

Intensity analysis. The analysis of earthquakes intensity based on the faulting characteristics, using empirical relationship between magnitude generation, allows determining the state of intensity; therefore, in this study we used equations (3) and (4) (Шебалин, 1961; Kuliyev, 1980), which allow determining the best-fit regional intensity scattering. Equation (3) generates the expected maximum magnitude due to the fault length (Fig. 5). Equation (4) generates the intensity for the area due to the expected maximum magnitude and depth of quake.

$$M = 2 * log\ (\mathrm{L}) + 2, \qquad (3)$$

$$I_0 = 1.5 * M - 3.3 * log\ (\mathrm{H}) + 2.7, \qquad (4)$$

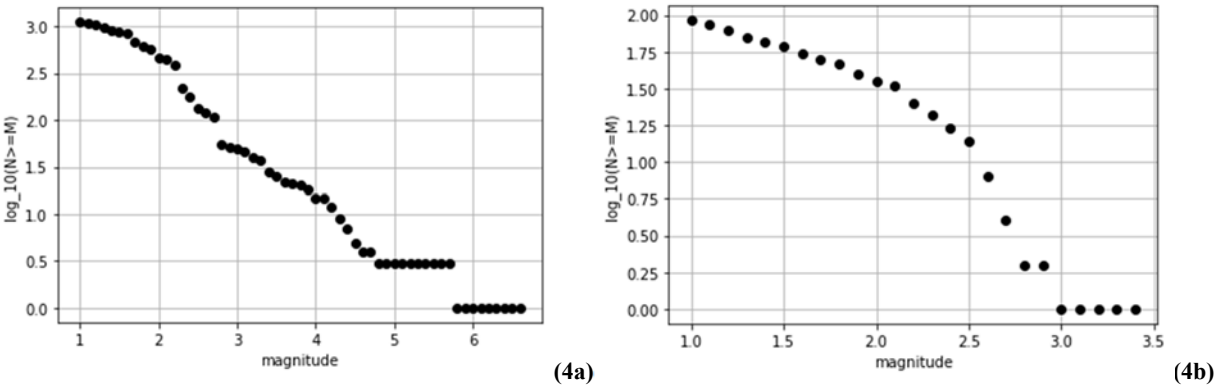


Fig. 4. Cumulative number of earthquakes in logarithmic scale against the magnitudes with N ≥ M with N – cumulative number of earthquakes and M – magnitudes (Gutenberg and Richter, 1942). (4a) Nº1, (4b) Nº2

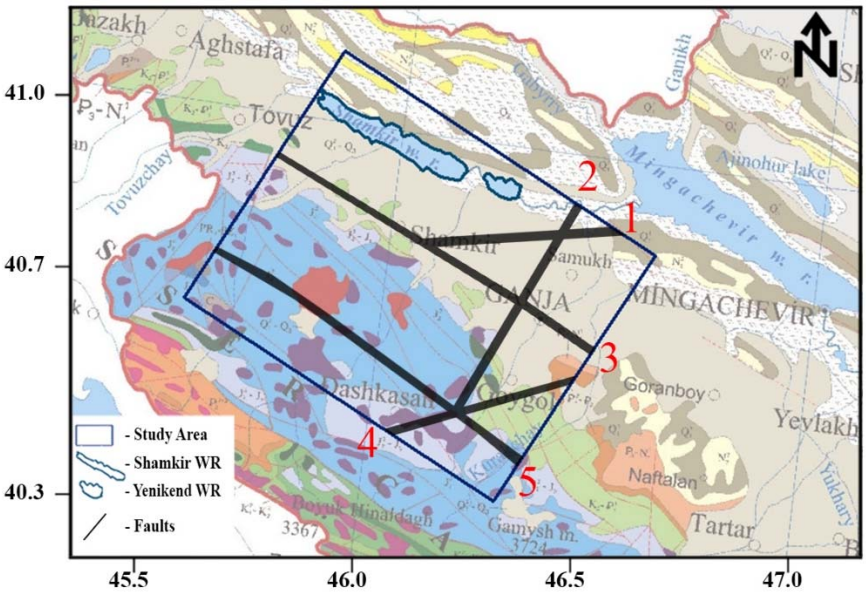


Fig. 5. Fault map of the study area
Note: Digits on the map refers to the enumeration of the faults, see Table 6

where M is maximum magnitude expected, L is the fault length and H is the depth of the earthquake with magnitude M.

Intensity shaking at the site of study in this research is determined from magnitude-fault relationship. This relationship is usually derived empirically from the motion database of past earthquakes. These relationships are simple functions of earthquake magnitude and source-site length with some additional source parameters-constants.

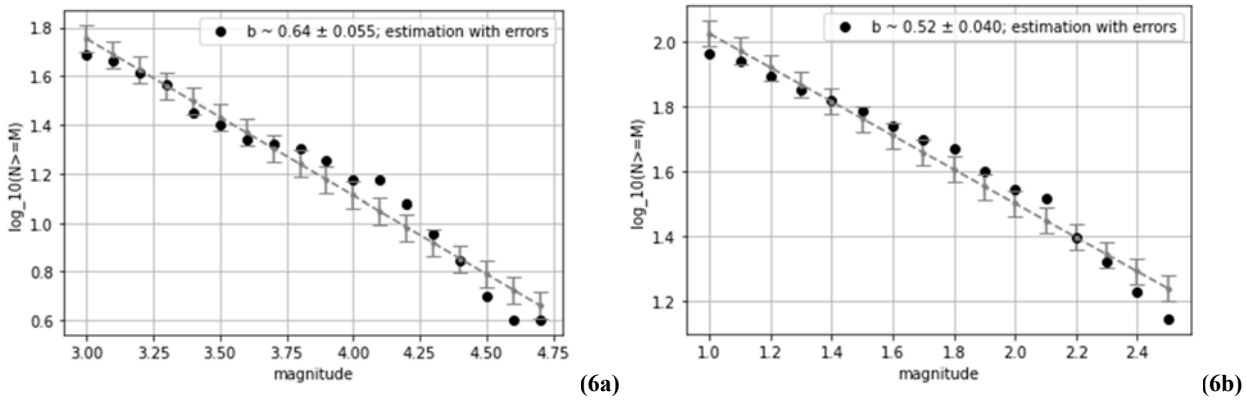
Results and Discussion

b-value estimation results. B- and a-values were obtained for each catalog applying linear least-square fitting (El-Isa, Eaton, 2014). B-value was at 0.64 and 0.52 and a-value was at 3.68 and 2.55 for the catalogs Nº1 and Nº2, respectively. The results of b-value are shown in Fig. 6 for both catalogs.

Seismicity analysis. Babayev et.al. (2020b) has shown that lower value of *b* represents higher activity of seismicity. Our results of b-value are more or less close to the b-values of the Shamakhi-Ismayilli and Zagatala regions presented by the mentioned study in which these zones were assessed relatively higher seismically active in the total area of the study due to the lower value of *b* (Babayev et al. 2020b; Babayev, Aliyev, 2019). Fig. 7 illustrates the spatial distribution of the earthquakes in both catalogs through the study area.

We observe relatively active seismicity in the northern and south-eastern parts of the study area. In the northern part, the activity is observed in the Shamkir and Yenikend water reservoirs which could be supposed that it is related to the seismicity of the Mingachevir water reservoir which is adjacent to the Shamkir and Yenikend water reservoirs by the Kur river (Telesca et.al., 2013), which are separately pre-

sented in Fig. 8b. Therefore, considering catalog Nº2 as a supporting argument (Fig. 8a), we could mention the triggering impact of the Mingachevir water reservoir (Telesca et.al., 2017) to the study area (Fig. 8b). Table 4 and 5 represent the extraction of earthquakes illustrated in Fig. 8b catalogs Nº1 and Nº2 respectively.



(6a) (6b)

Fig. 6. b-values for catalogs. (6a) Nº1, (6b) Nº2

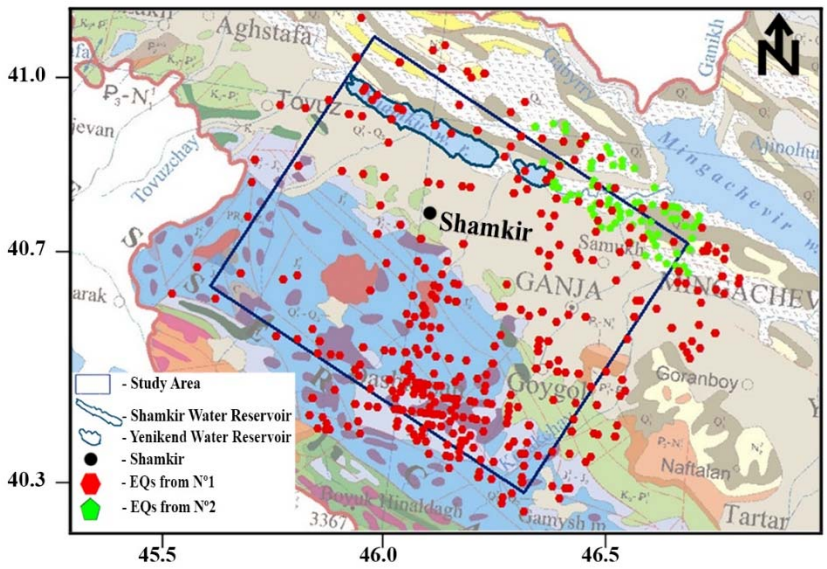
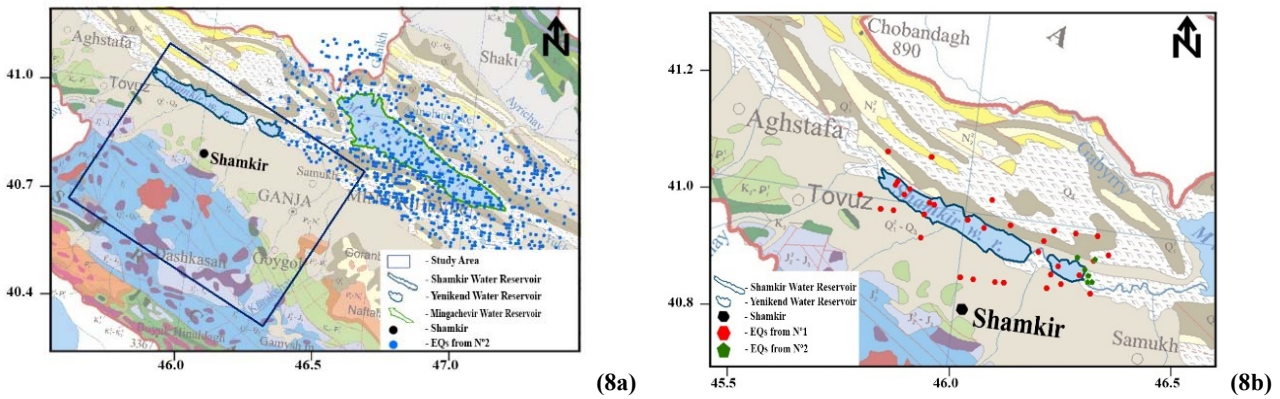


Fig. 7. Spatial distribution of the earthquakes through the study area. Dark blue frame borders the study area. Red hexagons represent earthquakes from catalog Nº1, green pentagons represent earthquakes from catalog Nº2



(8a) (8b)

Fig. 8. Earthquakes from catalogs occurred in the territory of the Shamkir and Yenikend water reservoirs or adjacent to them. (8a) All the events of Mingachevir catalog (Nº2) are distributed on the map

It is seen that the events are around the study frame that is considered as the impact of the Mingachevir water reservoir activity to the Shamkir water reservoir. Blue circles represent the earthquakes, (8b) red hexagons represent earthquakes from catalog Nº1, green pentagons represent earthquakes from catalog Nº2 that are in the study frame.

Table 4

Events from catalog Nº1 occurred in the territory of the Shamkir and Yenikend water reservoirs

Year	Lat	Lon	H (km)	Mlh	K
1962	41.0	45.9	5	4.20	11.6
1964	40.9	46.0	0	2.50	8.5
1964	40.9	46.0	0	2.50	8.5
1964	40.9	46.0	0	2.22	8.0
1964	41.0	46.1	0	1.67	7.0
1964	40.9	46.2	0	2.22	8.0
1965	41.0	45.8	0	2.78	9.0
1965	41.0	45.8	0	3.33	10
1966	41.0	46.1	0	2.78	9.0
1966	41.0	45.9	0	2.78	9.0
1968	41.0	45.8	0	2.78	9.0
1968	40.9	46.0	10	2.78	9.0
1968	41.1	45.9	0	2.78	9.0
1969	41.0	46.2	0	2.78	9.0
1971	40.9	46.2	0	2.78	9.0
1973	40.9	46.1	0	1.94	7.5
1973	40.9	46.2	0	2.50	8.5
1974	41.1	45.9	0	2.78	9.0
1974	41.1	45.9	0	2.78	9.0
1974	41.1	45.8	0	1.67	7.0
1976	40.9	46.0	0	1.67	7.0
1977	41.0	46.2	0	2.22	8.0
1977	41.1	45.9	0	3.33	10.0
1978	40.96	45.9	0	2.78	9.0
1979	41.1	45.8	25	3.33	10.0
1979	41.1	45.9	0	2.22	8.0
1979	41.1	45.8	0	1.67	7.0
1979	41.0	46.1	0	2.22	8.0
1980	40.9	46.3	0	2.78	9.0
1980	40.9	46.3	0	3.89	11.0
1980	40.9	46.3	0	1.67	7.0
1981	40.9	46.0	0	2.78	9.0
1981	41.0	46.3	0	2.78	9.0
1981	41.0	46.0	0	1.67	7.0
1981	41.0	46.2	20	2.78	9.0
1982	41.1	45.8	0	2.44	8.4
1982	41.0	46.0	0	2.22	8.0
1983	41.0	45.9	0	2.06	7.7
1983	41.0	45.9	0	2.00	7.6
1984	40.9	46.3	0	1.67	7.0
1984	41.0	45.8	0	1.67	7.0
1984	41.0	45.9	0	1.67	7.0
1985	40.9	46.0	0	2.33	8.2
1985	41.0	46.2	0	1.89	7.4
1985	40.9	46.2	0	2.78	9.0
1985	41.0	46.0	25	1.67	7.0
1985	41.1	45.9	0	2.56	8.6

Year	Lat	Lon	H (km)	Mlh	K
1985	40.9	46.1	0	2.33	8.2
1986	40.9	46.03	31	3.50	10.3
1986	41.1	45.8	0	1.67	7.0
1987	41.0	45.83	20	2.33	8.2
1987	40.91	46.23	30	2.50	8.5
1988	41.0	45.8	0	2.44	8.4
1988	40.9	46.0	0	1.89	7.4
1989	41.0	46.2	0	0.89	5.6
1989	41.1	45.8	0	2.06	7.7
1990	40.9	46.2	3	1.50	6.7
1990	41.0	46.0	0	1.89	7.4
1991	41.04	45.86	13	2.50	8.5
1991	40.9	46.08	1	1.44	6.6
1991	41.05	45.83	15	2.56	8.6
1991	40.94	46.22	0	1.78	7.2
1991	40.9	46.1	0	1.72	7.1
1992	41.0	45.8	0	2.22	8.0
1992	41.0	46.25	0	2.33	8.2
1993	40.99	46.04	22	2.39	8.3
1994	41.0	46.1	0	2.61	8.7
2000	40.9	46.1	0	2.22	8.0
2000	41.0	46.0	0	2.22	8.0
2000	40.93	46.27	22	3.06	9.5
2002	40.9	46.0	0	2.56	8.6
2002	40.96	46.17	11.7	2.11	7.8
2002	40.94	46.28	31	2.61	8.7
2004	41.04	46.05	24	2.06	2.8
2004	40.97	46.33	0	2.11	0
2007	40.98	46.18	0	1.56	0
2008	41.0	45.8	0	1.56	0
2013	41.02	45.91	13.63	2.35	0
2013	41.04	45.83	14.05	2.77	0
2014	40.96	46.3	11.1	2.15	0
2015	40.93	46.2	10.16	4.31	0
2015	41.02	45.92	10.0	2.58	0
2015	41.03	45.85	12	3.17	0
2015	41.02	45.75	14	2.11	0

Table 5

Events from catalog Nº2 occurred on the areas of the Shamkir and Yenikend water reservoirs

Year	Mon	Day	Hours	Second	Lat	Lon	H (km)	Ml
2002	12	5	10	40	40.94	46.28	31	2.80
2013	10	18	13	39	40.96	46.26	23	1.60
2014	12	16	18	18	40.96	46.30	11	2.20
2015	1	14	19	30	40.93	46.29	20	0.50
2015	3	5	0	44	40.92	46.30	13	1.10
2015	7	3	5	20	40.93	46.29	17	1.80
2018	8	3	21	26	40.92	46.29	11	1.13

As the b-value is a parameter describing seismicity analysis (Babayev et al., 2020b), we decided to estimate b-value in the three subdivisions of the study frame in order to verify our uncertainty about the variety of seismicity in the area. We divided the research zone into 3 parts roughly: the northern (Part I) – the part where the Shamkir and Yenikend water reservoirs are of main focus and the impact of Mingachevir zone is considered; the middle part (Part II) – where impact of the seismically active Ganja zone is

captured; and the southern part (Part III) – where seismicity of the Lesser Caucasus is examined (Fig. 9). During gridding the parts, the earthquakes were clustered respectively. As we clearly see that the events of Mingachevir catalog (Nº2) occur inside the Part I, we decided to merge those Mingachevir (Nº2) events to the events of Nº1 occurring in the same Part I. Thus, all the red and green quakes in Part I are clustered as the same group (Fig. 9).

After gridding of the area and clustering of the earthquakes, we re-estimated b-value. However, we changed M_c, M_{max}, bins for each part, necessarily, in order to get the best linear fitting. M_c, M_{max}, bins for the northern part are at 1.5, 4.5, 0.3, for the middle part – at 1.0, 5.0, 0.5 and for the southern part – at 3.0, 7.0, 1.0, respectively. b-values are at 0.72 for the northern, 0.59 for the middle and 0.32 for the southern parts accordingly. Fig. 10 illustrates the distribution map of b-values. Considering the result of Babayev et al. (2020b) which was a comparative analysis of seismicity with correlation of b-value, PGA (Peak Ground Acceleration) and Intensity (MSK-64), we adopt that seismicity relation between three divisions could be averaged and defined as follows: Part I < Part II < Part III.

Intensity analysis. Another goal of our study was to identify and to predict the intensity range of ground shaking that may occur from an earthquake at a particular magnitude along a fault. Consequently, an intensity (MSK-64) map for the study area was plotted (Fig. 11) applying equation (3) and (4). The faults capable of causing an event throughout the study area were listed in Table 6. Fig. 11 illustrates that intensity for the study area is estimated VII – VIII (MSK-64). Obviously, the area coinciding to the Lesser Caucasus zone has higher seismicity setting at VIII. However, intensity of VII that observed in the area of the Middle Kur depression also remarks a significant seismicity. This zone is under seismic impact of the seismically active territories such as Mingachevir from north-east, Ganja from south-east and Lesser Caucasus from the southern part.

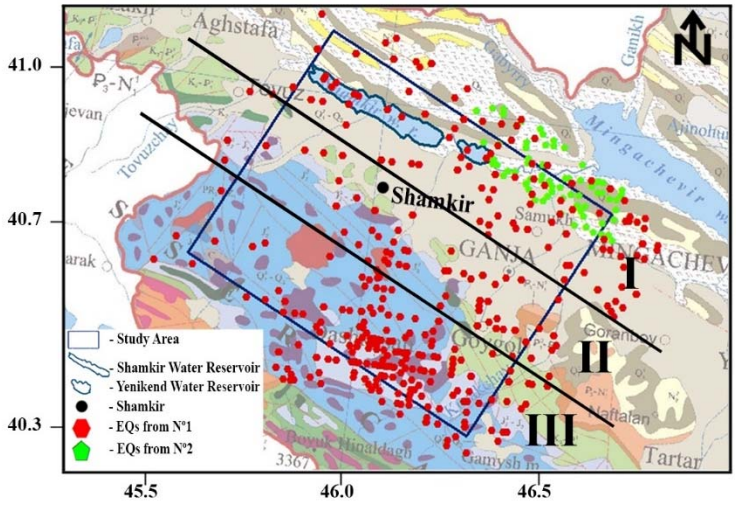


Fig. 9. The study area segmented into three parts in order to compute b-value spatial distribution

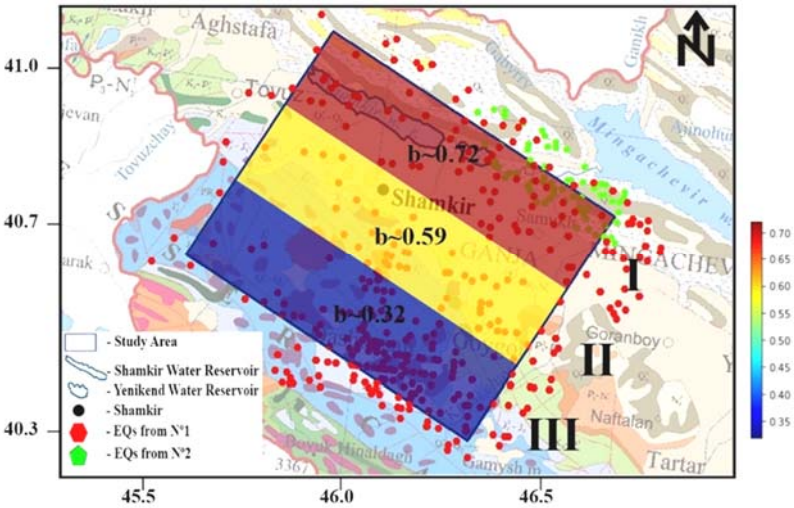


Fig. 10. Spatial distribution of b-value along the study area

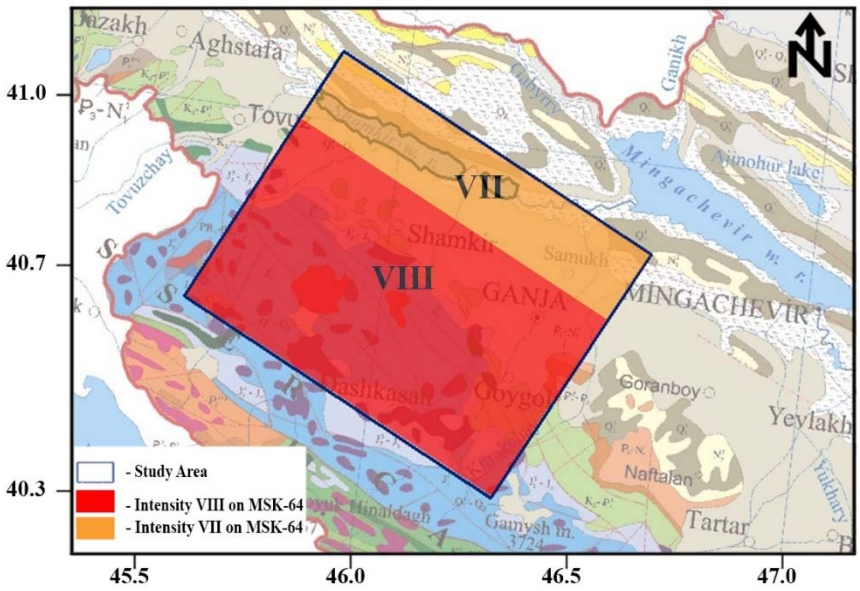


Fig. 11. Intensity (MSK-64) distribution map based on fault length along the study area

Table 6

Faults used to estimate intensity along the study area

N	L (km)	M	H (km)	I_0
1	39	5.2	10	7
2	48.8	5.4	10	7
3	73.7	5.7	10	8
4	36.4	5.1	10	7
5	74	5.7	10	8

Note: *Respective numeration of the faults (N) can be traced on the Fig. 5*

Conclusion

This study was dedicated to the seismicity analysis of the Shamkir water reservoir areas and adjacent territories using different tools. During the study, Gutenberg-Richter Law – b-value analysis and intensity estimation with faults of the region were applied. In terms of intensity analysis, the study zone was assessed of intensity VII-VIII (MSK-64) from north to south and in terms of b-value distribution, the study area is divided into three parts with b-values 0.72 for part I, 0.59 for part II and 0.32 for part III demonstrating seismically active character with the following regularity: part I < part II < part III. The intensity results indicate that, for engineering purposes this methodology can provide realistic ground-motion information in advance of an earthquake, including a model of what will actually happen.

Acknowledgments

The authors are thankful to the Republican Center of Seismic Survey at Azerbaijan National Academy of Sciences (ANAS) for providing earthquake catalogue. The study was performed at International Laboratory at Institute of Geology and Geophysics of the Ministry of Science and Education of the Republic of Azerbaijan and Institute of Methodologies for Environmental Analysis National Research Council (Italy) "Earthquake space-time analysis and hazard laboratory (ESTAHL)".

REFERENCES

Aliyev O.B. Stratigraphy and fauna of the cretaceous sediments of the north-eastern part of the Lesser Caucasus (between Qoshqarchay and Terterchay). AzSSR AN publishing house. Baku, 1961, 26 p. (in Russian).

Alizadeh A.A., Guliyev I.S., Kadirov F.A., Eppelbaum, L.V. Geosciences of Azerbaijan. Volume I: Geology, Cham: Springer. 2016, p. 340, https://doi.org/10.1007/978-3-319-27395-2.239.

Babayev G., Aliyev M. Seismic b-value study in southern slope of Greater Caucasus (Azerbaijan). Proceedings of the 2nd International Electronic Conference on Geosciences, 8-15 June 2019, MDPI: Basel, Switzerland, DOI: 10.3390/ IECG2019-06227.

Babayev G., Telesca L., Agayeva S., Ismail-zade T., Muradi I., Aliyev Y., Aliyev M. Seismic hazard analysis for southern

ЛИТЕРАТУРА

Alizadeh A.A., Guliyev I.S., Kadirov F.A., Eppelbaum L.V. Geosciences of Azerbaijan. Volume I: Geology, Cham: Springer. 2016, p. 340, https://doi.org/10.1007/978-3-319-27395-2.239.

Babayev G., Aliyev M. Seismic b-value study in southern slope of Greater Caucasus (Azerbaijan). Proceedings of the 2nd International Electronic Conference on Geosciences, 8-15 June 2019, MDPI: Basel, Switzerland, DOI: 10.3390/ IECG2019-06227.

Babayev G., Telesca L., Agayeva S., Ismail-zade T., Muradi I., Aliyev Y., Aliyev M. Seismic hazard analysis for southern slope of the Greater Caucasus (Azerbaijan). Pure and Applied Geophysics, Vol. 177 (8), 2020b, pp. 3747-3760, https://doi.org/10.1007/s00024-020-02478-0.

slope of the Greater Caucasus (Azerbaijan). Pure and Applied Geophysics, Vol. 177 (8), 2020b, pp. 3747-3760, https://doi.org/10.1007/s00024-020-02478-0.

Babayev G., Yetirmishli G., Kazimova S., Kadirov F., Telesca L. Stress field pattern in the northeastern part of Azerbaijan. Pure Appl. Geophys., Vol. 177(3), 2020a, pp. 2739-2751, Springer Nature Switzerland AS, https://doi.org/10.1007/s00024-019-02371-5.

Babayev T., Babayev G. Tectonic, geological, geomorphological and seismic analysis of Shamkir region and surroundings based on bibliographical review. Proceedings of Azerbaijan High Technical Educational Institutions (PAHTEI), Vol. 33(04), No. 10, 2023, pp. 73-81, DOI: 10.36962/PAHTEI33102023-73 (in Azerbaijani).

Bochud M. Tectonics of the Eastern Greater Caucasus in Azerbaijan. Thesis for: Phd n° 1733, Hauterive (Fribourg), Switzerland, 2011, 207 p.

El-Isa Z., Eaton D.W. Spatiotemporal variations in the b-value of earthquake magnitude–frequency distributions: Classification and causes. Tectonophysics, Vol. 615-616, 2014, pp. 1-11, http://dx.doi.org/10.1016/j.tecto.2013.12.001.

El-Isa Z.H. Continuous-cyclic variations in the b-value of the earthquake frequency-magnitude distribution. Earthquake Science, Vol. 26, 2013, pp. 301-320, https://doi.org/10.1007/s11589-013-0037-9.

ESRI. ArcGIS Desktop: Release 10.8. Environmental Systems Research Institute. Redlands: ESRI, 2018.

Felzer K. Calculating the Gutenberg-Richter b-value. USGS publication. 2007.

Godano C., Convertito V., Pino N.A. The signal to noise ratio and the completeness magnitude: the effect of the COVID-19 lockdown. Atmosphere, Vol. 12(5), 2021, 525, https://doi.org/10.3390/atmos12050525.

Godano C., Lippiello E., Arcangelis de L. Variability of the b value in the Gutenberg–Richter distribution, Geophysical Journal International, Vol. 199, No. 3, December 2014, pp. 1765-1771, https://doi.org/10.1093/gji/ggu359.

Gutenberg B., Richter C.F. Earthquake magnitude, intensity, energy and acceleration. Bulletin of the Seismological Society of America, Vol. 32, 1942, pp. 163-191.

Ishimoto M., Iida K. Observations sur les seismes enregistres parle microsismographe construit dernierement (1). Bulletin of the Earthquake Research Institute, Vol. 17, 1939, pp. 443-478.

Kadirov V.K. Gravity exploration in the study of geological structure and oil and gas content of Middle Kura depression of Azerbaijan. Journal of Geophysics (Geofizicheskiy jurnal), T. 34, No. 1, 2012, pp. 183-189 (in Russian).

Kulhanek O. Seminar on b-value. Prague Centre of Mathematical Geophysics, Meteorology and their Applications (MAGMA). Seminar paper, Department of Geophysics, Charles University. Prague, Czech, 2005.

Kuliev F.T. Macroseismic field equation of Azerbaijan. Seismological Bulletin of the Caucasus for 1977. Metsniereba.Tbilisi, 1980, pp.129-140 (in Russian).

Milojevic S. Power law distributions in information science: making the case for logarithmic binning. Journal of the American Society for Information Science and Technology, Vol. 61, 2010 No. 12, pp. 2417-2425, 10.1002/asi.21426.

Richter C.F. An instrumental earthquake magnitude scale. Bulletin of the Seismological Society of America, Vol. 25, No. 1, 1935, pp. 1-32.

Shebalin N.V. The intensity, magnitude and depth of the earthquake source. Earthquakes in the USSR, Nauka. Moscow, 1961, pp. 126-138 (in Russian).

Telesca L., Kadirov F., Yetirmishli G., Safarov F., Babayev G., Ismayilova S. Statistical analysis of the 2003-2016 seismicity of Azerbaijan and surrounding areas. Journal of Seismol-

Babayev G., Yetirmishli G., Kazimova S., Kadirov F., Telesca L. Stress field pattern in the northeastern part of Azerbaijan. Pure Appl. Geophys., Vol. 177(3), 2020a, pp. 2739-2751, Springer Nature Switzerland AS, https://doi.org/10.1007/s00024-019-02371-5.

Bochud M. Tectonics of the Eastern Greater Caucasus in Azerbaijan. Thesis for: Phd n° 1733, Hauterive (Fribourg), Switzerland, 2011, 207 p.

El-Isa Z., Eaton D.W. Spatiotemporal variations in the b-value of earthquake magnitude–frequency distributions: Classification and causes. Tectonophysics, Vol. 615-616, 2014, pp. 1-11, http://dx.doi.org/10.1016/j.tecto.2013.12.001.

El-Isa Z.H. Continuous-cyclic variations in the b-value of the earthquake frequency-magnitude distribution. Earthquake Science, Vol. 26, 2013, pp. 301-320, https://doi.org/10.1007/s11589-013-0037-9.

ESRI. ArcGIS Desktop: Release 10.8. Environmental Systems Research Institute. Redlands: ESRI, 2018.

Felzer K. Calculating the Gutenberg-Richter b-value. USGS publication. 2007.

Godano C., Convertito V., Pino N.A. The signal to noise ratio and the completeness magnitude: the effect of the COVID-19 lockdown. Atmosphere, Vol. 12(5), 2021, 525, https://doi.org/10.3390/atmos12050525.

Godano C., Lippiello E., Arcangelis de L. Variability of the b value in the Gutenberg–Richter distribution, Geophysical Journal International, Vol. 199, No. 3, December 2014, pp. 1765-1771, https://doi.org/10.1093/gji/ggu359.

Gutenberg B., Richter C.F. Earthquake magnitude, intensity, energy and acceleration. Bulletin of the Seismological Society of America, Vol. 32, 1942, pp. 163-191.

Ishimoto M., Iida K. Observations sur les seismes enregistres parle microsismographe construit dernierement (1). Bulletin of the Earthquake Research Institute, Vol. 17, 1939, pp. 443-478.

Kulhanek O. Seminar on b-value. Prague Centre of Mathematical Geophysics, Meteorology and their Applications (MAGMA). Seminar paper, Department of Geophysics, Charles University. Prague, Czech, 2005.

Milojevic S. Power law distributions in information science: making the case for logarithmic binning. Journal of the American Society for Information Science and Technology, Vol. 61, 2010, No. 12, pp. 2417-2425, 10.1002/asi.21426.

Richter C.F. An instrumental earthquake magnitude scale. Bulletin of the Seismological Society of America, Vol. 25, No. 1, 1935, pp. 1-32.

Telesca L., Kadirov F., Yetirmishli G., Safarov F., Babayev G., Ismayilova S. Statistical analysis of the 2003-2016 seismicity of Azerbaijan and surrounding areas. Journal of Seismology, Vol. 21, No. 6, 2017, pp. 1467-1485, https://doi.org/10.1007/s10950-017-9677-x.

Telesca L., Lovallo M., Babayev G., Kadirov F. Spectral and informational analysis of seismicity: An application to the 1996-2012 seismicity of Northern Caucasus–Azerbaijan part of Greater Caucasus–Kopet Dag Region. Physica A Statistical Mechanics and Its Applications, Vol. 392, No. 23, 2013, pp. 6064-6078, https://doi.org/10.1016/j.physa.2013.07.031.

Tibaldi A., Tsereteli N., Varazanashvili O., Babayev G., Barth,A., Mumladze T., Bonali F.L., Russo E., Kadirov F., Yetirmishli G., Kazimova S. Active stress field and fault kinematics of the Greater Caucasus. Journal of Asian Earth Sciences, Vol. 188, 2020, 104108, https://doi.org/10.1016/j.jseaes.2019.104108.

Utsu T. A method for determining the value of b in a formula log n = a – bM showing the magnitude–frequency relation for earthquakes. Geophys. Bull. Hokkaido Univ., Vol. 13, 1965, pp. 99-103.

ogy, Vol. 21, No. 6, 2017, pp. 1467-1485, https://doi.org/10.1007/s10950-017-9677-x.

Telesca L., Lovallo M., Babayev G., Kadirov F. Spectral and informational analysis of seismicity: An application to the 1996-2012 seismicity of Northern Caucasus–Azerbaijan part of Greater Caucasus–Kopet Dag Region. Physica A Statistical Mechanics and Its Applications, Vol. 392, No. 23, 2013, pp. 6064-6078, https://doi.org/10.1016/j.physa.2013.07.031.

Tibaldi A., Tsereteli N., Varazanashvili O., Babayev G., Barth,A., Mumladze T., Bonali F.L., Russo E., Kadirov F., Yetirmishli G., Kazimova S. Active stress field and fault kinematics of the Greater Caucasus. Journal of Asian Earth Sciences, Vol. 188, 2020, 104108, https://doi.org/10.1016/ j.jseaes.2019.104108.

Tskhakaya A.D. On depths of Caucasian earthquakes. Izv. Akad. Nauk SSSR, Ser. Geofiz., No. 5, 1962, pp. 577-584 (in Russian).

Utsu T. A method for determining the value of b in a formula log n = a – bM showing the magnitude–frequency relation for earthquakes. Geophys. Bull. Hokkaido Univ., Vol. 13, 1965, pp. 99-103.

Varazanashvili O.Sh. Seismic hazard assessment of Georgia by deterministic and probabilistic methods. Journal of Georgian Geophysical Society, Issue (A), Solid Earth, Vol. 4, 1999, pp. 35-45.

Varazanashvili O.Sh. Seismic hazard assessment of Georgia by deterministic and probabilistic methods. Journal of Georgian Geophysical Society, Issue (A), Solid Earth, Vol. 4, 1999, pp. 35-45.

Алиев О.Б. Стратиграфия и фауна меловых отложений северо-восточной части. Малого Кавказа. Автореф. диссерт. Изд-во АН АзССР. Баку, 1961, 26 с.

Гадиров В.Г. Гравиразведка при изучении геологического строения и нефтегазоносности площадей Среднекуринской впадины Азербайджана. Геофизический журнал, Т. 34, No. 1, 2012, с.183-189.

Кулиев Ф.Т. Уравнение макросейсмического поля Азербайджана. Сейсмологический бюллетень Кавказа за 1977 г. Мецниереба. Тбилиси, 1980, с. 129-140.

Цхакая А.Д. О глубинах кавказских землетрясений. Изв. Акад. Наук СССР, сер. Геофиз., No. 5, 1962, с. 577-584.

Шебалин Н.В. Балльность, магнитуда и глубина очага землетрясений. В кн.: Землетрясения в СССР. Наука. Москва, 1961, с. 126-138.

Babayev T., Babayev Q. Biblioqrafik icmal əsasında Şəmkir rayonu və ətrafının tektonik, geoloji, geomorfoloji və seysmik təhlili. Azərbaycan ali texniki məktəblərinin xəbərləri, cild 33 (04), No. 10, 2023, s. 73-81.

СЕЙСМИЧЕСКИЙ АНАЛИЗ ТЕРРИТОРИИ ШАМКИРСКОГО ВОДОХРАНИЛИЩА ПО ДАННЫМ ДИНАМИЧЕСКИХ ХАРАКТЕРИСТИК ЗЕМЛЕТРЯСЕНИЙ

Бабаев Т.Х., Алиев Я.Н., Муради И.Б., Алиев М.М.

Министерство науки и образования Азербайджанской Республики, Институт геологии и геофизики
AZ1143, Баку, просп. Г.Джавида, 119

Резюме. Данная статья посвящена анализу территории Шамкирского водохранилища с применением различных методов, используя каталоги землетрясений в качестве источника для долгосрочного анализа сейсмичности. Территория исследования охватывает западную часть Среднекуринской впадины и северо-восточную часть Малого Кавказа. Территория, занимающая 4300 км^2, находится под сейсмическим воздействием горных зон, таких как склон Большого Кавказа с севера и северо-восточная часть Малого Кавказа с юга. Анализ был проведен путем оценки значения b, характеризующий относительную величину распределения землетрясения. Для проведения исследований использовались два каталога землетрясений: с историческим периодом до 2015 года (№1) и инструментальным периодом с 1966 по 2018 годы (№2). Значение b было оценено путем определения M_c-уровня представительной магнитуды, M_{max} – максимальной магнитуды и пошаговой магнитуды по линейной зависимости Гутенберга-Рихтера. Для каталогов №1 и №2 было оценено значение b, равное 0.64 и 0.52 соответственно. Кроме того, в данной работе исследуется распределение интенсивности по активным разломам, генерирующим землетрясения, вычисленное с помощью эмпирической зависимости между максимальной магнитудой, которую может генерировать источник (разломы), и длиной источника (разломов). Интенсивность сотрясений в северной части территории доходит до отметки VII (MSK-64), а в южной части – до VIII баллов.

Ключевые слова: *Шамкирское водохранилище, Среднекуринская впадина, значение b, закон Гутенберга-Рихтера, интенсивность, движение грунта, сейсмотектоническая модель*

ZƏLZƏLƏLƏRİN DİNAMİK XÜSUSİYYƏTLƏRİNİN MƏLUMATLARINA ƏSASƏN ŞƏMKİR SU ANBARININ ƏRAZİSİNİN SEYSMİK TƏHLİLİ

Babayev T.H., Aliyev Y.N., Muradi I.B., Aliyev M.M.

Azərbaycan Respublikası Elm və Təhsil Nazirliyi, Geologiya və Geofizika Institutu
AZ1143, Bakı, G.Cavid prospekti, 119

Xülasə. Bu məqalə Şəmkir su anbarının ərazisinin uzunmüddətli seysmiklik səviyyəsinin təyin olunması üçün mənbə kimi zəlzələ kataloqlarından istifadə etməklə müxtəlif üsulların tətbiqi ilə təhlilinə həsr edilmişdir. Tədqiqat sahəsi Orta Kür çökəkliyinin qərb hissəsini və Kiçik Qafqazın şimal-şərq hissəsini əhatə edir. 4300 km^2 sahəni əhatə edən ərazi şimaldan Böyük Qafqaz yamacı və cənubdan Kiçik Qafqazın şimal-şərq hissəsi kimi dağlıq zonaların seysmik təsiri altında sıxılır. Təhlil zəlzələnin nisbi paylanma ölçüsünü təsvir edən b-qiymətinin hesablanması aparılmışdır. Tədqiqatın aparılması üçün iki zəlzələ kataloqundan istifadə edilmişdir: 2015-ci ilədək olan tarixi dövr (Nº1) və 1966-2018-ci illər arasında (Nº2) olan instrumental dövr. b-qiyməti hər bir kataloq üçün Qutenberq-Rixter xətti əlaqəsi üzrə Mc – maqnituda həddinin yekunlanma parametri, Mmax – maksimal maqnituda və interval – maqnituda intervallarını təyin edərək qiymətləndirilmişdir. Nº1 və Nº2 kataloqları üçün b-qiyməti müvafiq olaraq 0.64 və 0.52 hesablanıldı. Bundan əlavə, bu tədqiqat maksimal maqnituda və mənbənin (qırılmalar) uzunluğu arasındakı empirik əlaqə vasitəsilə hesablanmış, zəlzələləri əmələ gətirən qırılmaların xüsusiyyətlərinə əsasən intensivlik paylanmalarını araşdırır. Tədqiqat sahəsinin şimal hissəsində zəlzələnin intensivliyi VII (MSK-64), cənub hissəsində isə VIII ballıq müşahidə edilmişdir.

Açar sözlər: *Şəmkir su anbarı, Orta Kür çökəkliyi, b-qiyməti, Qutenberq-Rixter qanunu, intensivlik, yer hərəkəti, seysmotektonik model*